PROCEEDINGS, Twenty-Sixth Workshop on Geothermal Reservoir Engineering
Stanford University, Stanford, California, January 29-31, 2001
SGP-TR-168

ASSESSMENT OF HDR RESERVOIR GEOMETRY BY INVERSE MODELLING OF NON-LAMINAR HYDRAULIC FLOW

T. Kohl and L. Rybach

Institut für Geophysik
ETH-Hönggerberg
CH-8093 Zürich, Switzerland
e-mail: kohl@geo.phys.ethz.ch

ABSTRACT

At the GPK1 and GPK2 boreholes of the HDR test site Soultz-sous-Forêts (F) the hydraulic properties have been extensively investigated. Especially the multiple level flow rate injection or production experiments conducted between 1994 and 1997 in the open hole sections identified the complex hydraulic regime. A common observation in these tests has been that the downhole pressure response attained quasi-steady state levels within a few days and that the duration of the transient pressure variation seemed to be a function of the flow rate. In attempting a quantitative interpretation of these pressure records, the importance of turbulent-like hydraulic behavior became evident. In the past, forward techniques have been adopted to simulate these experiments. The 2-D models allowed excellent fits to be accomplished assuming non-Darcian flow in the fracture network.

Multi-dimensional, inverse modeling procedures are applied for the transient data fit which allow to extract more sophisticated information from these numerical models. Thereby, not only the correlation or sensitivity of individual model parameters but also the confidence interval can be quantified. The results identify matrix diffusivity and fracture aperture as the most sensitive parameters. Further, special attention was paid to constrain the reservoir geometry. Therefore, the distance of the far-field reservoir boundaries which seem to coincide with permeable faults systems was assessed as function of possible flow geometries (parallel flow paths, impedance distribution along flow paths or tortuous flow). These studies improve and assist other methods in developing a conceptual model of the situation in the ~3.5 km deep Soultz reservoir.

INTRODUCTION

The observation and interpretation of the hydraulic flow regime in fractured rock provide important hints for the characterization of the flow paths behind the borehole wall. It is especially a crucial factor for developing operation strategies for Hot Dry Rock (HDR) systems which involve essentially forced flow of cool fluid (>30 l s^{-1}) injected into a hot fractured rock between two or more boreholes. At such high rates, the flow velocity in the individual fractures can be extremely high (>1 m s^{-1}). Experience obtained from world-wide HDR research highlighted the need to better understand the processes that influence the flow field within the reservoir fracture system.

The development of non-laminar flow regime has been originally investigated for pipes (e.g. Blasius 1913) and later for fractures (e.g. Lomize 1951, Louis 1967). A summary on existing laboratory flow experiments in fractures is given by Kohl et al. (1997) who also highlighted the discrepancy between the rather large interest in laboratory investigations on non-laminar flow behavior in fractures and the small number of field investigations. Furthermore, they described the constitutive relationship developed employed for non-laminar flow analysis. For a comprehensive presentation of the actual study this derivation will be shortly outlined adopting Louis'(1967) originally used units. Along a vertical fracture 1-D non-Darcian flow regime can be described by

$$Q/H = -a \cdot \tilde{K} \cdot \sqrt{\nabla h}$$

or

$$Q^2 = H^2 \cdot a^2 \cdot \tilde{K}^2 \cdot \nabla h \qquad (1)$$

where

$$\tilde{K} = \sqrt{32 \cdot a \cdot g} \cdot \log\left(\frac{1.9}{e/D_h}\right)$$

with ∇h is the gradient of piezometric head, *Q/H* the flow rate per unit height of a vertical fracture, *a* the aperture of the fracture, ε the mean absolute height of the asperities and D_h the hydraulic diameter. Substituting Louis' law into the continuity equation yields a description for the transient hydraulic field for 1-D flow between two rough fracture surfaces:

$$S_S \cdot \frac{\partial h}{\partial t} = \nabla \cdot \left(\tilde{K} \cdot \sqrt{\nabla h} \right)$$

with S_s the specific storage coefficient and t the time.

INVERSE MODELLING PROCEDURE

The inverse modeling approach used here is based on the forward modeling procedure applied in Kohl et al. (1997). The finite element code FRACTure (Kohl & Hopkirk, 1995) has been used for the purpose of forward simulation of non-laminar fluid flow. The computer program UCODE (Poeter & Hill 1998) has been used in combination with the forward code FRACTure. The UCODE approach for inverse modeling and statistical methods can be broadly applied to various existing numerical or analytical programs. In combination UCODE and FRACTure perform inverse modeling, posed as a parameter-estimation problem, by calculating parameter values that minimize a weighted least-squares objective function using nonlinear regression. Minimization during the backward simulation is accomplished using a modified Gauss-Newton method. The inverse modeling procedure of UCODE is described in detail by Hill (1998) and will be only shortly outlined.

The weighted least-squares objective function *S(b)* is a measure of the fit between simulated values and the observations that are being matched by the regression. Ignoring any prior information it can be expressed as:

$$S(\underline{b}) = \sum_{i=1}^{ND} w_i [y_i - y'_i(\underline{b})]^2$$

where, $\underline{b}$ is a vector containing values of each of the *NP* parameters being estimated, *ND* is the number of observations, y_i is the ith observation being matched by the regression, y'_i is the simulated value which corresponds to the ith observation, and w_i is the weight for the ith observation. By the regression values of defined parameters are calculated that minimize the objective function or the residuals $[y_i - y'_i(b)]$. The simulated values related to the observations are of the form $y'_i = f(\underline{b},x)$, where b and ξ are independent variables such as fracture aperture and time, with the function f being calculated by the numerical model. Alternatively the least-squares objective function can be derived from the maximum-likelihood objective function (Carrera and Neuman, 1986). Assuming a normalized common error variance the value of the maximum-likelihood objective function is calculated as:

$$S'(\underline{b}) = ND \ln 2p - \ln |\underline{?}| + (\underline{y} - \underline{y'})^T \underline{?} (\underline{y} - \underline{y'})$$

where $\underline{\omega}$ is the determinant of the weight matrix.

A key information in inverse modeling is the sensitivity analysis which allows to determine confidence intervals. UCODE assumes the procedure described by Hill (1992) with scaled sensitivities being calculated for diagonal weight matrices by:

$$ss_{ij} = \left(\frac{\partial y'_k}{\partial b_j} \right) b_j \sqrt{w_{ii}}$$

where b_j is the jth estimated parameter and $\partial y'_k / \partial b_j$ is the sensitivity of the simulated value associated with the *kth* observation with respect to the *jth* parameter. Clearly, because of the nonlinear problem the value of a sensitivity will be different for different values of $\underline{b}$.

HYDRAULIC MULTI-RATE EXPERIMENTS

The European HDR project site Soultz s.F. is located about 60 km north of Strasbourg (France). Situated in a Graben structure the Soultz area is transversed by several large N-S striking faults, parallel to the trend of the Graben structure. The Soultz area was selected as HDR test site mainly for its high local surface temperature gradient (up to 100°C km^{-1}) and heat flow (above 0.150 W m^{-2}).
Currently two deep boreholes are drilled at Soultz, GPK1 (~3800 m) and GPK2 (~5000 m). A temperature of nearly 200°C was encountered in the borehole GPK2 at current bottom hole depth. During different project phases several depth ranges of both boreholes have been investigated by numerous hydraulic experiments. In the analysis presented herein we focus on single borehole experiments performed between 1994 and 1996 in the GPK1 and GPK2 borehole. At that time the open hole depth range of GPK1 was 2850 - 3590m and of GPK2 was 3211 - 3876 m. In all described experiments, pressure will be referred to as downhole differential pressure, ΔP, which corresponds to the difference between the measured downhole pressure and the natural formation pressure. This pressure remained at least 4 MPa below the minimum stress component (i.e. below the pressure required for jacking).

The four multi-rate flow experiments which are investigated herein will be described in the following sections. All hydraulic experiments presented here were conducted at multiple pressure or flow rate steps, i.e. flow rate or pressure was held constant until quasi steady-state conditions were approached, after which a new level was established. Pressure was measured by downhole gauges whereas flow rate was measured at the wellbore head.

Hydraulic tests 94JUN16 (GPK1)

After a major stimulation of the open hole section during which a total volume of 45'000 m^3 has been

injected into the host rock a multi rate production test has been performed in June 1994. This 94JUN16 experiment lasted 12 days. Fluid was produced at constant drawdown levels (1.0, 0.3 and 0.7 MPa) which led after a period of two days to approximately steady-state flow rates (~11, 5 and 7 l s^{-1}). At the Soultz site production can be established due to formation artesian pressure (0.15 MPa) and to buoyancy in the borehole and was realised in 94JUN16 by controlling the venting of GPK1 with a throttle valve. This hydraulic production tests consisted three flow rate steps (-1 MPa, -0.3 MPa and –0.7 MPa) performed during 12 days in June 1994 (94JUN16). Near steady-state conditions were attained for the -0.3 and -0.7 MPa production level (see Fig. 2). The hydrostatic pressure at 2830 m was measured before the 94JUN16 test at 28.63 MPa.

Hydraulic tests 94JUL04 (GPK1)

The production experiment was followed in July by an 8 days injection test (94JUL04). During the 94JUL04 test constant injection flow rates (6, 12 and 18 l s^{-1}) were used which led to a quasi steady state pressure increase at the first two steps (0.4, 1.7 MPa) but continuous transient behavior of the last step (see Fig. 3).

Hydraulic tests 95JUL01 (GPK2)

After the end of major stimulation injections (28'000 m^3 were injected into the open hole section) in GPK2, a hydraulic test 95JUL01 with multiple flow rates was performed during four days in July 1995. In this 95JUL01 experiment injection flow rates of approx. 6, 13, 19 and 26 l s^{-1} were used. Due to the shorter step period, compared to the 1994 series in GPK1, strongly transient pressure records were obtained (see Fig.4). Automatic monitoring of the downhole pressure failed during the first and part of the second flow step and had to be corrected by the hand registration. Hydrostatic pressure was found to be at 32.32 MPa at 3200 m depth.

Hydraulic tests 96SEP29 (GPK2)

In 1996, GPK2 was subjected to a second stimulation with flow rate up to 79 l/s (Baumgärtner et al. 1996). After a one week period it was followed by a step-rate injection test into GPK2 (96SEP29) with GPK1 shut-in to evaluate the impact of the stimulation. Flow rates of 6.2, 15.5 25 and 37.3 l s^{-1} were used which led to transient influenced pressure drawdowns of 0.5, 1.55, 3.6 and 6.8 MPa (see Fig.5).

INVERSE MODELING OF MULTI-PRESSURE LEVEL HYDRAULIC EXPERIMENTS

Background

It has been shown by Kohl et al. (1996) for the 95JUL01 experiment and Kohl et al. (1997) for the 94JUN16 / 94JUL04 experiment that the pressure records show the typical pattern for non-laminar flow behavior. This can be identified for quasi-steady state levels by the fact that

1) steady state pressure change is not linear to flow rate but rather $\Delta h \propto Q^2$ and
2) transient time interval to reach steady state depends on flow rate $\Delta t = f(Q)$

In Kohl et al. (1996 & 1997) these phenomena have been simulated using the FRACTure code with rather simple model geometries. This reflects the fact that the physical behavior of non-laminar flow needed to be identified and that the model could only be fitted by a relative small number of representative elementary volumes (REV's). They used the following three REV's: (1) the borehole, (2) a single conduit characterized by a turbulent-like (non-Darcian) flow regime and (3) a rock matrix with Darcian flow regime. A key feature in these models is the inclusion of high-capacity reservoir faults which are connected to the borehole by the hydraulic conduit. The existence of such features is supported by geological evidence (Elsass, 1995) as well as by the observed total and immediate loss of drilling mud in a jointed zone near 2000 m during the drilling of the GPK2 borehole. It should be emphasized that the existence of these reservoir faults are essential for the justification of this successful modeling approach since they provide a direct (non-divergent) flow path and a far field drainage system. The influence of these faults becomes obvious by the fact that steady–state conditions are attained already after a few days. Additionally, in a divergent flow pattern around the borehole, the flow would tend to switch into Darcian flow regime at some distance from the borehole which should become visible by the data analysis. It is to be shown that non-Darcian flow occurs even at larger distance from the borehole.

Model constraints

Automated inverse modeling theoretically allows to define more complex and probably more realistic structures. Problems of instability and nonuniqueness represent however major problems in inverse modeling and obtaining useful results depends on (1) defining a tractable inverse problem using simplifications appropriate to the system under

investigation and (2) sensitivity analysis using the statistics generated and the match between observed and simulated values, and associated graphical analyses.

Therefore a careful variation of the initial model geometry has been attempted. Now, different assumptions on the nature of the flow between the borehole and the far field fault were taken. Flow in the matrix always is assumed to be Darcian.

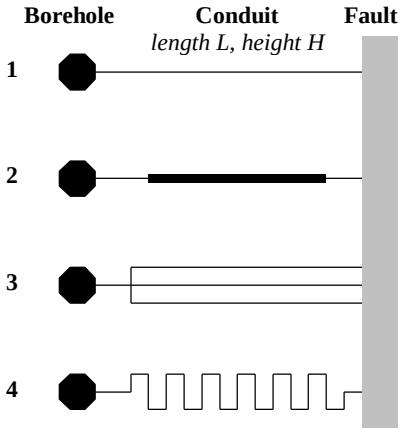

Fig. 1: Plane view to the different model assumptions for the main flow field between borehole and far field fault. All flow paths are embedded in a Darcian rock matrix of height H. The thin lines illustrate non-Darcian flow behavior (see text for details).

The following scenarios were considered (see also Fig. 1):

1) non-laminar flow between borehole and fault ("initial model")
2) non-laminar behavior manifesting close to the borehole and due to channeling effects near the fault systems. Low impedance flow occurs in the intermediate zone with irrelevant Darcian or non-Darcian nature. ("variable flow")
3) the non-laminar conduit splits near the borehole into three parallel flow paths ("parallel flow")
4) the non-laminar conduit has an approximately 3 times larger effective path length than the direct distance between borehole and fault ("tortuous flow")

For each model assumption a fit of the measured pressure record was intended with a variable length, height and matrix diffusivity. The fitting parameter is aperture and matrix storage coefficient, S_{sM}. Earlier analysis has shown that due to its physically reasonable bounds especially the evaluation of the non-linear S_{sM} parameter allows a quantification of reservoir geometry. Its lower bound may be estimated to be ~$8x10^{-11}Pa^{-1}$ based on the compressibility of water (~$5x10^{-10}$ Pa^{-1}), the compressibility of rock (~$10^{-11}Pa^{-1}$, Evans et al. 1992) and on the fact that adjacent fractures will increase the overall system storativity. Although the fracture system in Soultz is nearly vertical, an upper bound can be calculated from the matrix overloading.

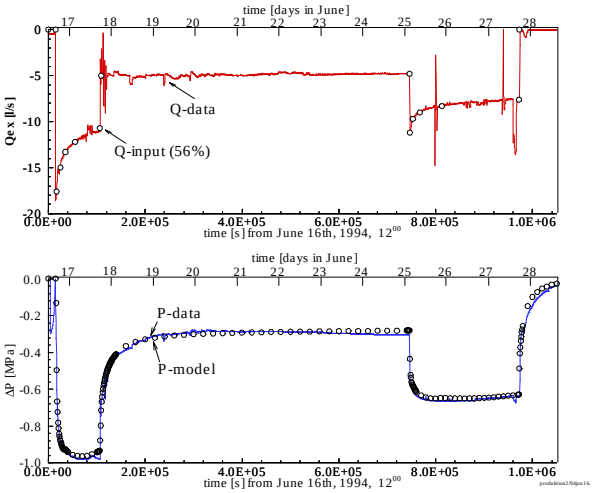

Fig. 2: 94JUN16 production test: Flow rate (top) and differential pressure in GPK1 (bottom) Measurements are given by continuous lines and simulations by open circles.

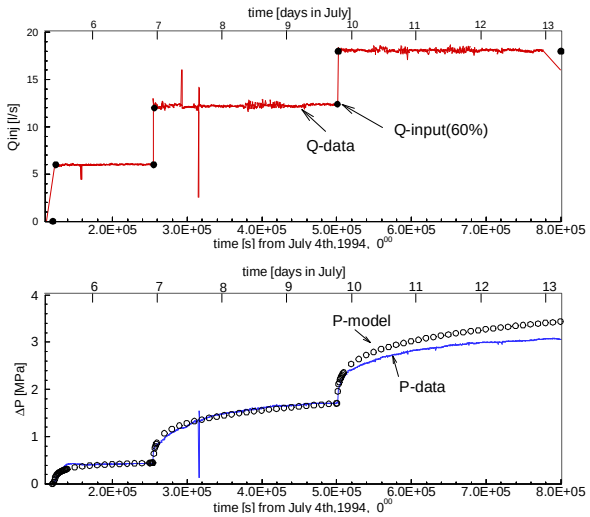

Fig. 3: 94JUL04 injection test: Simulated and measured flow rate (top) and differential pressure in GPK1 (bottom)

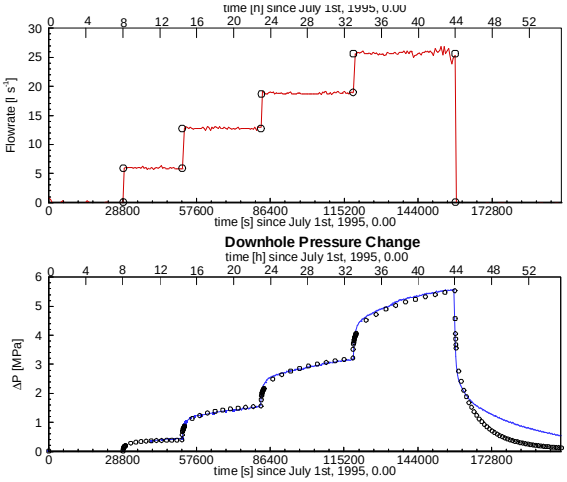

Fig. 4: 95JUL01 injection test in GPK2.

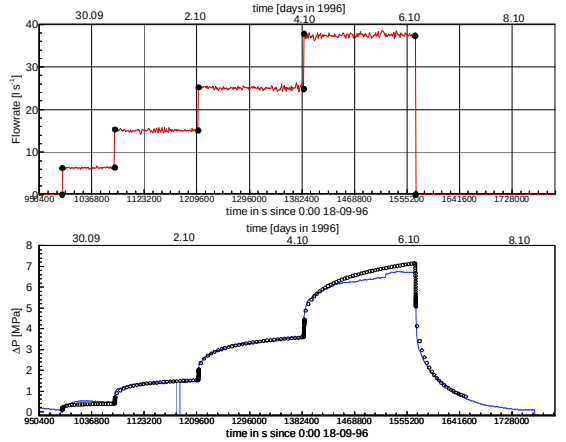

Fig. 5: GPK2 stimulation characterization experiment 96SEP29

Simulation results

In the inverse modeling procedure all four experiments have been considered for every model assumption from Fig. 1. It was intended to achieve similar good quality fits like those shown in Figs.2-5. For the inversion each pressure record had to be discretized into an arbitrary number of "observations" which each a given standard deviation. The general standard deviation provided to all other observations is 0.1 MPa. The observation points were taken at very small spacings close to a change in flow rate which continuously increased the closer steady-state conditions were reached.

The parameters which could be estimated are matrix permeability, *k*, matrix storage coefficient, S_{sM}, fracture aperture, *a*, length of the conduit, *L*, and height of the conduit, *H*. Initial calculations failed which intended to predict several of these parameters. Especially, the strong correlation between matrix permeability and storage coefficient which was close to "1" should be noted for all experiments. Furthermore, matrix permeability and fracture aperture, also showed less pronounced but still evident correlation. Therefore, it was decided to assume for all experiments a constant matrix permeability of $10^{-15}m^2$ which has been determined by thermal model fits (e.g. LeCarlier et al. 1994) and constant fluid viscosity of $10^{-3}Pa^{-1}\ s^{-1}$ (except for the 94JUN16 production experiment with $2x10^{-4}Pa^{-1}\ s^{-1}$). Further effect on the model prediction is provided by the geometrical extensions L and H which are also closely related (see equation 1 with $\tilde{N}h \gg Dh/DL$). Therefore, good parameter estimation could only be achieved for the two parameters matrix storage coefficient, S_{sM}, fracture aperture, *a*, but constant k and L/H ratios. For the case of the "variable flow" model with a L = H = 100 m and constant *k*, the estimated parameters for S_{sM} and *a* are shown in Fig 6.

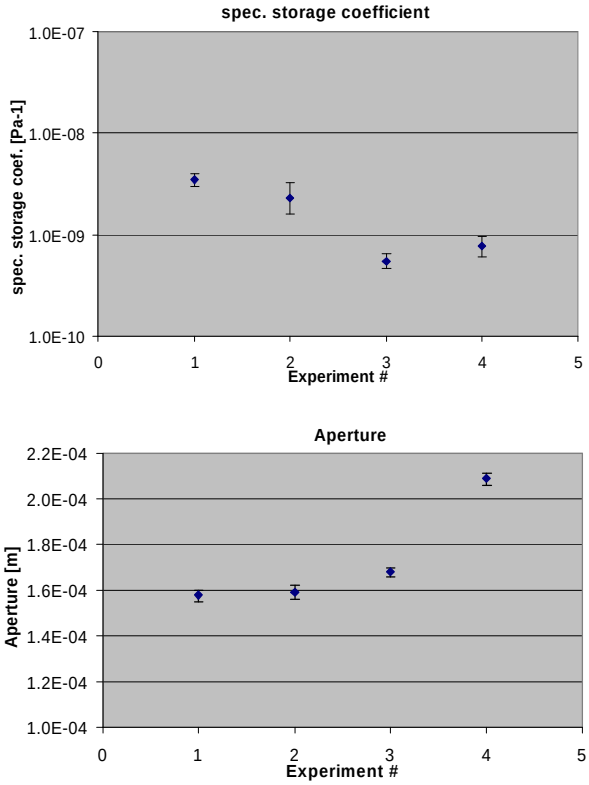

Fig. 6: Estimated "S_{sM}" and "a" parameters for a given geometry (see text) of all 4 experiments (#1 corresponds to 94JUN16, #2 to 94JUL04, #3 to 95JUL01 and #4 to 96SEP29). Also plotted are the corresponding 95% confidence intervals of the model prediction.

It is obvious from Fig. 6 that both GPK1 tests, the production experiment 94JUN16 and the injection experiment 94JUL04, show nearly identical results. This fact can be considered to be a proof for the strength of the methodology used, since the experimental layout of these tests was completely different. Another important result can be observed

for the 94JUL04 injection experiment: here, rather large 95% confidence intervals result. This is due to the fact that the last step of this experiment (see Fig. 3) is generally rather poorly matched. Since it has been decided that the full experiment cannot be simulated by a pure hydraulic model (mechanical interaction!) the observations for this last step were defined with a four times larger standard deviation in order not to influence the results of the first two steps.

Another fact which is obvious from Fig. 6 are the nearly identical S_{sM} values for the two GPK2 experiments but the strong variation of the aperture values. The reasoning behind these results is the hydraulic stimulation between the 95JUL01 and the 96SEP29 experiment. This stimulation has resulted in an increased injectivity (or larger fracture aperture) but should not affect the matrix storage value.

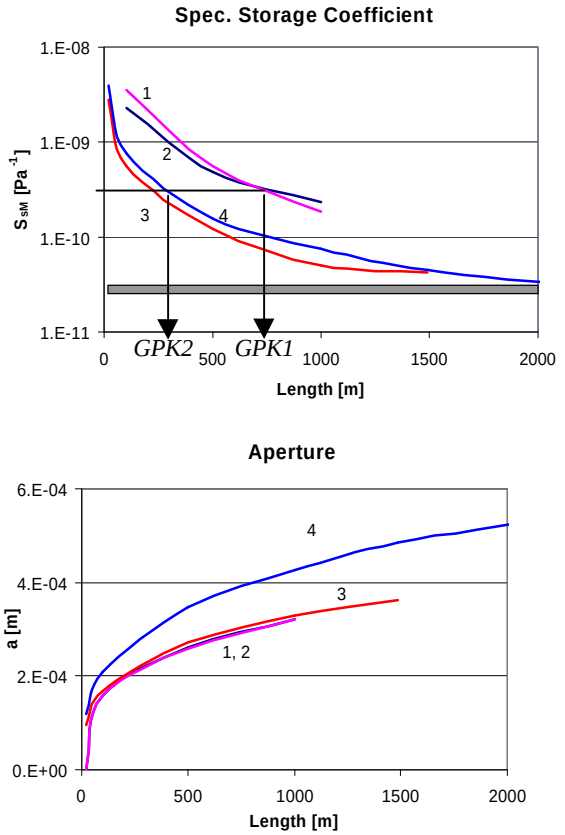

Fig. 7: Variation of "S_{sM}" and "a" parameters at different lengths but constant model height (H=100 m) for the case of the "variable flow" model. #1 corresponds to 94JUN16, #2 to 94JUL04, #3 to 95JUL01 and #4 to 96SEP29.

The same behavior is seen in Fig. 7 which shows the influence of different model lengths (i.e. the distance from borehole to the far-field faults) but constant model height (H=100 m) to the parameter estimations for the case of the "variable flow" model. Evidently, the S_{sM} values for the GPK1 experiments and the S_{sM} values for the GPK2 experiments are each nearly identical at all investigated geometries (Fig. 7 top). Also the difference between the fracture aperture calculated for the two GPK1 experiments is so small that it cannot be seen on the scale of Fig. 7 (bottom). Clearly, the analysis shows the largest aperture for the 96SEP29 experiment.

Under the hypothesis of an uniform specific storage coefficient for the rock matrix in the ~3500 m deep Soultz reservoir this analysis allows a quantification of the relative distance of GPK1 and GPK2 boreholes to the far field fault. When assuming a value of $5x10^{-9}Pa^{-1}$ it can be depicted from Fig. 7 that GPK2 has a smaller distance to a far field fault than GPK1, in this case by approximately a factor of "0.5". Clearly, given other S_{sM} values or other matrix models the absolute value for the length L will change. It is however evident from the other model runs that the same conclusion is valid for all model calculation. It also seems to be a reasonable conclusion since during drilling of GPK2 a fault zone has been hit at ~2200 m depth.

CONCLUSION

The hydraulic behavior in the fractured granitic Soultz reservoir is clearly determined by non-laminar flow. Earlier evaluations (Kohl et al. 1996 & 1997) have shown that the downhole pressure records in GPK1 or GPK2 cannot be explained by a significant laminar flow. Several alternative flow models have been evaluated in this presentation which offer more realistic prospects to the subsurface flow field and which all can explain the measurements. Their common feature non-laminar flow in a conduit and a far-field highly conductive fault system. In contrast to many other geothermal sites, such faults are an integral part of a reservoir but the same time they represent its boundaries.

The inverse modeling procedure which combines the two codes UCODE and FRACTure has been successfully applied for the non-laminar flow analysis. Herewith, it became possible to automate earlier trial-and-error type analysis and to calculate numerous different models. Besides the characterization of flow geometry the results allows to quantify a strategy for hydro-tests. The 94JUN16 data set is particularly suited for sensitivity analysis because the alternating high and low flow rates strongly depend on matrix diffusivity. The analysis of this test always showed the lowest correlation between individual parameters and therefore has the highest confidence. It is suggested for future tests that a similar alternating strategy is applied to future high-rate flow experiments in fractured rock.

REFERENCES

Baumgärtner, J., R. Jung, A. Gérard, R. Baria, and J. Garnish, 1996, The European HDR project as Soultz-sous-Forêts: Stimulation of the second deep well and first circulation experiments, in 21st Stanford Workshop on Geothermal Reservoir Engineering, Stanford University, Stanford, California, pub. Stanford University, 267-274

Blasius H., 1913, Das Ähnlichkeitsgesetz bei Reibungsvorgängen in Flüssigkeiten, Mitteilungen über Forschungsarbeiten Ingenieurwesen, 134, Berlin
Elsass P., 1995, Deep structures of the Soultz-sous-Forêts HDR site, Proc. World Geothermal Congress, Florence, Italy, pp 2543-2647

Carrera, J. & Neuman, S.P., 1986, Estimation of aquifer parameters under transient and steady-state conditions: Water Resources Research, v.22, no. 2, p. 199-242.

Evans, K. F., T. Kohl, R. J. Hopkirk, and L. Rybach, 1992, Modelling of energy production from Hot Dry Rock systems, Final Report to Swiss National Energy Research Fund, Swiss Federal Institute of Technology/Polydynamics, NEFF 359, April 1992.

Evans, K.F., 2000, The effect of the 1993 stimulations of well GPK1 at Soultz on the surrounding rock mass: Evidence for the existence of a connected network of permeable fractures, Proc. World Geothermal Congress,May 28th-June 10th, 2000, Sendai, Japan, 3695-3700.

Hill, M.C., 1992, A computer program (MODFLOWP) for estimating parameters of a transient, three-dimensional, ground-water flow model using nonlinear regression: U.S. Geological Survey Open-File Report 91-484, 358 p.

Hill, M.C., 1998, Methods and guidelines for effective model calibration, U.S. Geol. Survey, Water-Resources Investigations Report 98-4005

Kohl T., R. Jung, R. J. Hopkirk & L. Rybach, 1996, Non-linear flow transients in fractured rock masses - The 1995 injection experiment in Soultz, Proc. 21st Workshop Geothermal Reservoir Engineering, Stanford Univ. CA, USA, 22-24 Jan. 1996, 21, pp.157-164

Kohl T., K.F. Evans, R.J. Hopkirk, R. Jung & L. Rybach, 1997, Observation and simulation of non-Darcian flow transients in fractured rock, Water Resources Research, 33(3), pp.407-418.

LeCarlier C., J.J. Royer & E.L. Flores, 1994, Convective heat transfer at the Soultz-sous-Forêts Geothermal Site: Implications for oil potential, First Break, 12, No.11, 553-560

Lomize G.M., 1951, Water flow in fissured rocks, (in Russian), Gosenergoizdat, Moscow

Louis C., 1967, Strömungsvorgänge in klüftigen Medien und ihre Wirkung auf die Standsicherheit von Bauwerken und Böschungen im Fels, PhD Thesis, Institut für Bodenmechanik & Felsmechanik, 30, Univ. Karlsruhe, Germany, (Translated in English by Univ. of California, UCRL-Trans-10469)

Nikuradse, J., 1933, Strömungsgesetze in rauhen Rohren, Mitteilungen über Forschungsarbeiten Ingenieurwesen, 361 Berlin

Poeter E. P. & Hill M. C., 1998, Documentation of UCODE, A Computer Code for Universal Inverse Modeling, U.S. Geological Survey, Water-Resources Investigations Report 98-4080